Unique morphological characteristics of mitochondrial subtypes in the heart: the effect of ischemia and ischemic preconditioning

Siavash Beikoghli Kalkhoran[1,2], **Peter Munro**[3], **Fan Qiao**[4], **Sang-Bing Ong**[5,6], **Andrew R. Hall**[1,2], **Hector Cabrera-Fuentes**[5,6,7,8], **Bibhas Chakraborty**[4], **William A. Boisvert**[9], **Derek M. Yellon**[1,2], and **Derek J. Hausenloy**[1,2,5,6,10,11,*]

[1]Hatter Cardiovascular Institute, University College London, UK

[2]National Institute of Health Research University College London Hospitals Biomedical Research Ctr., UK

[3]Institute of Ophthalmology, University College London, UK

[4]Centre for Quantitative Medicine, Duke-NUS Graduate Medical School, Singapore

[5]Cardiovascular and Metabolic Disorders Program, Duke-National University of Singapore

[6]National Heart Research Institute Singapore, National Heart Centre Singapore

[7]Kazan Federal University, Department of Microbiology, Kazan, Russian Federation

[8]Escuela de Ingenieria y Ciencias, Centro de Biotecnologia-FEMSA, Tecnologico de Monterrey, Mexico

[9]Center for Cardiovascular Research, John A. Burns School of Medicine, University of Hawaii

[10]Yong Loo Lin School of Medicine, National University Singapore, Singapore

[11]Barts Heart Centre, St Bartholomew's Hospital, London, UK

Abstract

Rationale—Three subsets of mitochondria have been described in adult cardiomyocytes - intermyofibrillar (IMF), subsarcolemmal (SSM), and perinuclear (PN). They have been shown to differ in physiology, but whether they also vary in morphological characteristics is unknown. Ischemic preconditioning (IPC) is known to prevent mitochondrial dysfunction induced by acute myocardial ischemia/reperfusion injury (IRI), but whether IPC can also modulate mitochondrial morphology is not known.

Aims—Morphological characteristics of three different subsets of adult cardiac mitochondria along with the effect of ischemia and IPC on mitochondrial morphology will be investigated.

*Corresponding author: Derek J. Hausenloy, MD, Cardiovascular & Metabolic Diseases Program, Duke-NUS Graduate Medical School Singapore, 8 College Road, Singapore 169857; derek.hausenloy@duke-nus.edu.sg; Phone: +65 65166719;.

Conflict of Interest:
The authors declare no conflicts of interest.

Methods—Mouse hearts were subjected to the following treatments (N=6 for each group): stabilization only, IPC (3x5 min cycles of global ischemia and reperfusion), ischemia only (20 min global ischemia); and IPC and ischemia. Hearts were then processed for electron microscopy and mitochondrial morphology was assessed subsequently.

Results—In adult cardiomyocytes, IMF mitochondria were found to be more elongated and less spherical than PN and SSM mitochondria. PN mitochondria were smaller in size when compared to the other two subsets. SSM mitochondria had similar area to IMF mitochondria but their sphericity measures were similar to PN mitochondria. Ischemia was shown to increase the sphericity parameters of all 3 subsets of mitochondria; reduce the length of IMF mitochondria, and increase the size of PN mitochondria. IPC had no effect on mitochondrial morphology either at baseline or after ischemia.

Conclusion—The three subsets of mitochondria in the adult heart are morphologically different. IPC does not appear to modulate mitochondrial morphology in adult cardiomyocytes.

INTRODUCTION

There are three distinct sub-populations of mitochondria present in adult cardiomyocytes: Intermyofibrillar (IMF) mitochondria, which reside between the myofibers and mainly provide energy for myocardial contraction; subsarcolemmal (SSM) mitochondria that are localized beneath the plasma membrane and provide energy for ion channel function; and perinuclear (PN) mitochondria that are juxtaposed to the cell nucleus and mainly provide energy for gene transcription[1,2]. These 3 mitochondrial subtypes in the heart have been shown to differ in function in terms of oxidative capacity, calcium uptake and sensitivity to mitochondrial permeability transition (MPTP) opening[3–7]. In spite of the presence of large volume of literature concerning the physiology of cardiac mitochondria, the morphological differences between the 3 mitochondrial subtypes have not been comprehensively investigated in the adult heart.

Changes in mitochondrial morphology and function have been shown to be critical to the susceptibility of the heart to acute ischemia/reperfusion injury (IRI), and the cardioprotective phenomenon of ischemic preconditioning (IPC), an intriguing phenomenon in which one or more cycles of brief ischemia and reperfusion render the myocardium tolerant to lethal IRI[8–10]. The mechanisms underlying IPC have been extensively investigated and comprise a complex array of signal transduction pathways many of which converge on and preserve the function of mitochondria following acute IRI. A number of prosurvival kinases implicated in IPC signaling such as AKT and PKA have been shown to modulate the mitochondrial function[11,12]. Hence, it is plausible to hypothesize that IPC induces its cardioprotective effect by modulating the morphology of cardiac mitochondria.

In this study, we investigate the morphological differences between the three subtypes of mitochondria in adult murine cardiomyocytes and investigate the changes induced by

ischemia. We then investigate the effect of IPC on mitochondrial morphology at baseline and following ischemia.

MATERIALS AND METHODS

Experimental procedures were performed in accordance to the Animals (Scientific Procedures) Act 1986 published by the UK Home Office. Hearts obtained from male 8–10 weeks old C57/BL6 mice were used throughout.

Langendorff

Mouse hearts were extracted after the induction of euthanasia (Sodium Pentobarbitone (20mg/ml)) and were cannulated and perfused with Krebs-Henseleit buffer containing NaCl (118 mM), $NaHCO_3$ (25 mM), d-Gluocose (11 mM), KCl (4.7 mM), $MgSO_{4.7}H_2O$ (1.22 mM), KH_2PO_4 (1.21 mM) and $CaCl_2.H_2O$ (1.84 mM) on a constant pressure Langendorff setup gassed with 95% O_2-5% CO_2, pH 7.35–7.45. Hearts were randomly allocated four different treatment groups (N=6 for each group) and were subjected to either:

a.   55 minutes of stabilization (ST)

b.   25 minutes of stabilization and IPC protocol of 3x cycles of 5 minutes ischemia/5 minutes reperfusion (ST+IPC)

c.   55 minutes of stabilization and 20 minutes of ischemia (ST+ IS)

d.   25 minutes of stabilization and 30 minutes of IPC followed by 20 minutes of ischemia (ST+IPC+IS) as shown in Figure 1.

TEM specimen processing and imaging

Hearts were fixed using EM grade 1% paraformaldehyde, 2% glutaraldehyde in 0.1M sodium cacodylate buffer. Sections from left ventricle were obtained from the hearts and were post-fixed using 2% osmium tetraoxide for 2 hours at 4°C. Each segment then underwent sequential dehydration using different concentration of ethanol (25%, 50%, 70%, 90%, 100%) and washed with 1,2-epoxypropane, before being embedded in Epoxy resin (Poly/Bed-21844-1). Ultrathin sections of 70nm were cut using an ultra-microtome (Reichert) and were further stained using lead citrate. Images were acquired using a Jeol 1010 transmission electron microscopes equipped with Gatan Orius and had a pixel dimensions of 5 x 5 nm in both X and Y. For each subtype of mitochondria in each heart, 6 representative cells in their longitudinal orientation were captured in a blinded fashion. In total, 7,301 IMF mitochondria, 5,346 PN mitochondria and 3739 mitochondria were segmented and analyzed. Cells with intact fibers were selected for the analysis and hypercontracted cells as well as cells with myofibrillar disarray were excluded from the analysis.

Image analysis

Three subsets of cardiac mitochondria were segmented and traced using image J (V. 1.47). Shape descriptors of individual mitochondria were measured in 2D including:

a.   "surface area (expressed as μm^2)";

b. "perimeter (the distance surrounding the actual shape of mitochondria in 2D, expressed in μm)";

c. "aspect ratio (AR) (representing major to minor axis ratio)";

d. "Feret's diameter (defined as the longest distance between any two points within the selected mitochondrion, expressed in μm)";

e. "roundness (calculated by the formula: 4 x Area/π x Major axis^2)"; and

f. "circularity (calculated by the formula: 4π x Area/Perimeter^2). Mitochondria exhibiting a perfect circular shape have a circularity value close to 1.0 whereas more elongated mitochondria have a circularity value that is closer to 0.0)".

Statistics

All statistical tests were performed using Stata (v.13). Mitochondrial shape descriptors were analyzed using the mixed effects model with random effects accounting for variability among cells and hearts of the nested structure, and the fixed effects of mitochondrial types or different treatments. Mitochondrial Area and AR were logarithmically transformed in order to perform the analysis on normally distributed data. Graphs illustrating model-predicted means and 95% confidence intervals were made using Microsoft Excel 2010. Box and whiskers plot, illustrating the median and 5% to 95% percentile, were used to show frequency distribution of individual shape descriptors. p value of 0.05 was considered significant.

RESULTS

Morphological Differences of Three Subtypes of Cardiac Mitochondria

The precise location of cardiac mitochondria determines their morphological constitution[13]. In mouse cardiac myocytes IMF mitochondria are often rectangular and are extended between the myofibers allowing them to make contact with their two juxtaposed mitochondria (indicated by white arrows in Figure 2) whereas SSM mitochondria reside by the subsarcolemmal region and form clusters that are less organized than the IMF mitochondria (indicated by black arrows in Figure 2).

Similarly, PN mitochondria also form clusters around the nucleus of cardiac myocytes and extend between the myofibers but lack the typical elongated morphology of IMF mitochondria (indicated by yellow arrow and star in Figure 2).

Morphological comparisons of different subsets at ST indicated that the IMF mitochondria are not larger than SSM mitochondria (Figure 3a), however, they have significantly larger perimeter (Figure 3b), which corresponds to their rectangular shape and greater Feret's diameter (Figure 3c). These facts are also evident from the distribution of shape descriptors of these two individual subtypes (see Supplementary Figure 1).

In addition, the rounder (Figure 3d) and more circular shape (Figure 3e) of SSM mitochondria as well as their lower AR (Figure 3f) and perimeter (Figure 3b) makes this subtype less elongated than IMF mitochondria. Moreover, PN mitochondria are smaller in

respect to area (Figure 3a); shorter in terms of perimeter (Figure 3b) and Feret's diameter (Figure 3c) when compared to the other two mitochondrial subtypes. Lower AR (Figure 3f) as well as higher roundness (Figure 3d) and circularity (Figure 3e) also indicates that the mitochondria belonging to this subtype are not branched and extended to the other region of cardiomyocytes and instead interacts with their neighboring mitochondria thereby permitting faster inter-mitochondrial communication (refer to Supplementary Figure 1 for distributions of individual subsets). Collectively, these data indicate the presence of three morphologically disparate subtypes of mitochondria in adult cardiac mitochondria.

Pronounced alteration in morphology of IMF mitochondria in response to ischemia

IMF mitochondria are known to be less sensitive to ischemia in comparison to SSM mitochondria[5,14]. IPC itself does not have any significant effect on morphology of IMF mitochondria (Figures 4a, 4b and 5) and the distribution of their shape descriptors (Supplementary Figure 2); however, IPC alters the intermyofibrillar space and the level of mitochondrial compactness between the intermyofibrillar regions as shown in Figure 4b. The compactness of myofibers is further disrupted upon the induction of ischemia and IPC treatment given prior to ischemia does not prevent the occurrence of this alteration (Figure 4c and 4d). Further, this change is accompanied by a shift in distribution patterns of individual mitochondrial shape descriptors shown in Supplementary Figure 2. Ischemia induces a dramatic 11% reduction in Feret's diameter (Figure 5c) and 27% increase in roundness of IMF mitochondria (Figure 5d). Although mitochondrial area does not change after ischemia (Figure 5a), the presence of significant changes in mitochondrial circularity (Figure 5e) and AR (Figure 5f) as well as a non-significant trend towards a decrease in mitochondrial perimeter (Figure 5b) further hints to the magnitude of ischemia-induced fragmentation in this subtype. Lastly, the absence of significant shape differences between the groups which received ischemia with or without IPC, shown in Figure 5, suggests that the morphological alterations of IMF mitochondria after ischemia are not preserved by the IPC treatment

Shape changes in SSM mitochondria

SSM mitochondria maintain their condensed network after individual treatments while losing their elongated morphology (Figure 6). Phenotypic alterations are substantially less evident in SSM mitochondria in comparison to IMF after the IPC only treatment (Figure 6a and 6b). However, SSM mitochondria receiving ischemia only or IPC before the ischemia show an extensive increase in rotundity (See Figure 6c and 6d). In parallel to the data from IMF mitochondria, IPC only treatment does not induce any significant changes in shape parameters and their distribution in SSM mitochondria (Figure 7 and Supplementary Figure 3).

Morphometric evaluation of the groups receiving ischemia with or without IPC point to the absence of any changes in SSM mitochondria in terms of area and perimeter of all treatment groups (Figure 7a, 7b and Supplementary Figure 3). Unlike IMF mitochondria, ischemia alone does not change the Feret's diameter of SSM mitochondria whereas hearts receiving IPC before ischemia exhibit a significant reduction of Feret's diameter (Figure 7c). In

addition, no significant differences are observed in terms of Feret's diameter between groups receiving ischemia with or without IPC (Figure 7c).

In line with sphericity data of IMF mitochondria, ischemia alone induces a 13% rise in roundness of SSM mitochondria (Figure 7d). This in turn is accompanied by the reduction of AR (Figure 7f) and an increase in circularity (Figure 7e) thereby indicating a reduction of elongated SSM mitochondria after ischemia. In parallel to the data from IMF mitochondria, IPC given prior to ischemia does not induce any meaningful significant changes in respect to the morphology of SSM mitochondria after ischemia (Figure 7 & Supplementary Figure 3).

PN mitochondria respond differently to ischemia and IPC

Perinuclear mitochondria are the least studied mitochondria in adult cardiac myocytes. EM micrographs of PN mitochondria undergoing IPC-only treatment illustrate an absence of any substantial positional and morphological changes (Figure 8a, 8b). In comparison, PN mitochondria from the ischemia-only group or ischemia group receiving IPC exhibit larger as well as more circular PN mitochondria (Figure 8c and 8d - yellow arrows). Besides, a distinct loss of endoplasmic reticulum structure around the nuclear region is evident in these ischemic groups (Figure 8c, 8d). PN mitochondria do not exhibit morphological alterations after IPC only treatment (Figure 9 and Supplementary 4). In contrast to the morphometric data from SSM and IMF, an increase in PN mitochondrial area (Figure 9a) can indicate potential swelling of PN mitochondria following ischemia. Besides, IPC treatment given prior to ischemia (Figure 9a) does not prevent the significant rise in the area and perimeter of this subset (Figure 9a and 9b). Together, with the lack of any significant difference in respect to perimeter and Feret's diameter of the two ischemic groups (Figure 9b and 9c) these data indicate the absence of any modulating effect of IPC on PN mitochondria. Moreover, the increase in roundness (Figure 9d), circularity (Figure 9f and 9e) and AR (Figure 9f) of PN mitochondria additionally demonstrate that the morphological alterations induced by ischemia are not altered by IPC (see Supplementary Figure 4 for the distributions of individual parameters).

CONCLUSION

In this study, we showed for the first time that the three subsets of mitochondria in the adult heart differ in their morphological characteristics and respond differently to ischemic stress. We also found that IPC had no effect on mitochondrial morphology at baseline and following ischemia. Subtype heterogeneity of cardiac mitochondria in terms of physiology and morphology has been described to be critical for the effective response to pathological stimuli and is highly preserved in mammals[2,15–19]. Although the role of mitochondrial morphology in cellular physiology has become clearer in recent years, the exact morphological behavior of cardiac mitochondria under normal and pathological settings have not been comprehensively studied and are For mainly confined to IMF and SSM mitochondria[13,20–23]. Furthermore, the morphological status of mitochondria within cells are directly linked with their function[24,25] instance, H2O2 insult of neonatal rat ventricular myocytes induces a dysregulation of Ca^{2+} handling and dissipation of mitochondrial membrane potential which in turn increases the measure of mitochondrial roundness[26].

Similarly, IRI simulation in H9C2 cells has been shown to induce the formation of circular donut shaped mitochondria which possess lower membrane potential and altered K^+ cannel activity in comparison to their elongated counterparts which further supports the link between the morphology of mitochondria and their function[27]. Consistent with our findings, a study of myocardial cells isolated from the monkey's heart showed that the perinuclear mitochondria are the least elongated and most spherical subtype of mitochondria present in cardiac myocytes. Interestingly, the same group also showed that the SSM mitochondria are longer in diameter than the other subtypes of mitochondria whereas our study showed a greater diameter in IMF mitochondria in comparison to other subtypes[18]. The shape differences that we observed between SSM and IMF mitochondria of cardiac myocytes are also present in the same subtypes in mouse skeletal muscle cells. Skeletal muscle SSM mitochondria are shorter in respect to perimeter and Feret's diameter as well as being rounder in comparison to IMF mitochondria. However, both SSM and IMF mitochondria from skeletal muscle mitochondria are shorter in respect to Feret's diameter and perimeter compared with the same subtypes of cardiac mitochondria[17]. Collectively, these studies stress that the shape differences observed in different subtypes of cardiac mitochondria are influenced by their regional location. Moreover, the presence of differences in terms of shape parameters of same subtypes of mitochondria further emphasizes on the extent of species and cell-specific nature of mitochondrial morphology.

The unique metabolic and potential structural differences between various subtypes of cardiac mitochondria appear to mediate subtype-specific feedback in response to IRI as well as cardioprotective strategies conducted against this insult including IPC. For instance, an induction of global no-flow ischemia in rabbit hearts can hamper SSM oxidative phosphorylation whereas the IMF mitochondria remains unaffected[28]. Isolated SSM mitochondria from male Sprague Dawley rats also exhibit lower oxidative phosphorylation and reduced NADH oxidation after a 40 minutes hypoxia/reoxygenation insult thereby indicating the unique properties of mitochondrial subtypes[21]. Likewise and in partial agreement with our data, myocardial infarction via left coronary artery ligation of male Sprague Dawley rats has been shown to specifically alter the topography[29]. In parallel, IPC has been shown to induce its cardioprotective effects by increasing the S-nitrosylation, promoting the complex I respiration and preserving the activity of electron transport chain enzymes of SSM mitochondria[30,31]. These results indicate the importance of both morphology and physiology of different mitochondrial subtypes in cardiomyocytes function.

Major impairment of mitochondrial structure begins before the induction of reperfusion and during ischemia and preserving the abrupt fragmentation has been shown to confer cardioprotection[32–35]. Nevertheless, the mechanism behind morphological alterations of different subtypes of cardiac mitochondria following acute ischemia is poorly understood. In line with previous reports, we observed granulation and increase in mitochondrial roundness in all subtypes of mitochondria; however, only PN mitochondria showed significant swelling after ischemia[36,37].

Our results are consistent with our previous report where we showed a decrease in the length of IMF mitochondria after treating mouse hearts with 20 minutes of ischemia[34].

Within the same report we also showed that the mitochondria division inhibitor can preserve the morphology of IMF mitochondria thereby indicating the therapeutic potential of manipulating this subtype of cardiac mitochondria[34]. Moreover, preservation of mitochondrial morphology via IPC has been previously shown to confer cardioprotection in the setting of IRI[11,38–40]. Although IPC has been suggested to preserve the function of SSM mitochondria following IR, we did not observe any IPC-induced preservation of SSM mitochondria morphology following ischemia-only treatment[30,31]. The absence of shape-preservation in all subtypes of cardiac mitochondria in our study may indicate that the possible protective effects of IPC on mitochondrial morphology are not mediated during ischemia, but are actually initiated at the start of reperfusion.

In conclusion, we show for the first time that the three subsets of cardiac mitochondria have unique shape parameters. Ischemia induced morphological alterations in all three subsets of cardiac mitochondria and its effects were not rescued by IPC.

Supplementary Material

Refer to Web version on PubMed Central for supplementary material.

Acknowledgments

Abbreviations

IMF	Intermyofibrillar mitochondria
SSM	Subsarcolemmal mitochondria
PN	Perinuclear mitochondria
TEM	Transmitted electron microscopy
IPC	Ischemic preconditioning
MPTP	Mitochondrial permeability transition pore
ST	Stabilization
EM	Electron microscopy
AR	Aspect ratio
S.E	Standard error

References

1. Ong S-B, Hall AR, Hausenloy DJ. Mitochondrial dynamics in cardiovascular health and disease. Antioxid Redox Signal. 2013; 19(4):400–14. [PubMed: 22793879]

2. Hollander JM, Thapa D, Shepherd DL. Physiological and structural differences in spatially distinct subpopulations of cardiac mitochondria: influence of cardiac pathologies. Am J Physiol Heart Circ Physiol. 2014 Jul 1; 307(1):H1–14. [PubMed: 24778166]

3. Palmer JW, Tandler B, Hoppel CL. Biochemical differences between subsarcolemmal and interfibrillar mitochondria from rat cardiac muscle: effects of procedural manipulations. Arch Biochem Biophys. 1985 Feb; 236(2):691–702. [PubMed: 2982322]

4. Suh JH, Heath S-H, Hagen TM. Two subpopulations of mitochondria in the aging rat heart display heterogenous levels of oxidative stress. Free Radic Biol Med. 2003 Nov 1; 35(9):1064–72. [PubMed: 14572609]

5. Holmuhamedov EL, Oberlin A, Short K, Terzic A, Jahangir A. Cardiac subsarcolemmal and interfibrillar mitochondria display distinct responsiveness to protection by diazoxide. PLoS One. 2012; 7(9):e44667. [PubMed: 22973464]

6. Palmer JW, Tandler B, Hoppel CL. Biochemical differences between subsarcolemmal and interfibrillar mitochondria from rat cardiac muscle: effects of procedural manipulations. Arch Biochem Biophys. 1985 Feb 1; 236(2):691–702. [PubMed: 2982322]

7. Gustafsson R, Tata JR, Lindberg O, Ernster L. The relationship between the structure and activity of rat skeletal muscle mitochondria after thyroidectomy and thyroid hormone treatment. J Cell Biol. 1965 Aug; 26(2):555–78. [PubMed: 5893687]

8. Murry CE, Jennings RB, Reimer KA. Preconditioning with ischemia: a delay of lethal cell injury in ischemic myocardium. Circulation. 1986 Nov; 74(5):1124–36. [PubMed: 3769170]

9. Cabrera-Fuentes HA, Aragones J, Bernhagen J, Boening A, Boisvert WA, Bøtker HE, et al. From basic mechanisms to clinical applications in heart protection, new players in cardiovascular diseases and cardiac theranostics: meeting report from the third international symposium on "New frontiers in cardiovascular research". Basic Res Cardiol. 2016 Nov.111(6):69. [PubMed: 27743118]

10. Cabrera-Fuentes HA, Alba-Alba C, Aragones J, Bernhagen J, Boisvert WA, Bøtker HE, et al. Meeting report from the 2nd International Symposium on New Frontiers in Cardiovascular Research. Protecting the cardiovascular system from ischemia: between bench and bedside. Basic Res Cardiol. 2016 Jan.111(1):7. [PubMed: 26667317]

11. Kamga Pride C, Mo L, Quesnelle K, Dagda RK, Murillo D, Geary L, et al. Nitrite activates protein kinase A in normoxia to mediate mitochondrial fusion and tolerance to ischaemia/reperfusion. Cardiovasc Res. 2014 Jan 1; 101(1):57–68. [PubMed: 24081164]

12. Ong S-B, Hall AR, Dongworth RK, Kalkhoran S, Pyakurel A, Scorrano L, et al. Akt protects the heart against ischaemia-reperfusion injury by modulating mitochondrial morphology. Thromb Haemost. 2015 Mar; 113(3):513–21. [PubMed: 25253080]

13. Palmer JW, Tandler B, Hoppel CL. Biochemical properties of subsarcolemmal and interfibrillar mitochondria isolated from rat cardiac muscle. J Biol Chem ASBMB. 1977 Dec; 252(23):8731–9.

14. Shin G, Sugiyama M, Shoji T, Kagiyama A, Sato H, Ogura R. Detection of mitochondrial membrane damages in myocardial ischemia with ESR spin labeling technique. J Mol Cell Cardiol. 1989 Oct; 21(10):1029–36. [PubMed: 2555524]

15. Birkedal R, Shiels Ha, Vendelin M. Three-dimensional mitochondrial arrangement in ventricular myocytes: from chaos to order. Am J Physiol Cell Physiol. 2006 Dec; 291(6):C1148–58. [PubMed: 16822946]

16. Fawcett DW, McNutt NS. The ultrastructure of the cat myocardium. I. Ventricular papillary muscle. J Cell Biol. 1969 Jul; 42(1):1–45. [PubMed: 4891913]

17. Picard M, White K, Turnbull DM. Mitochondrial morphology, topology, and membrane interactions in skeletal muscle: a quantitative three-dimensional electron microscopy study. J Appl Physiol. 2013 Jan; 114(2):161–71. [PubMed: 23104694]

18. Shimada T, Horita K, Murakami M, Ogura R. Morphological studies of different mitochondrial populations in monkey myocardial cells. Cell Tissue Res. 1984; 238(3):577–82. [PubMed: 6525619]

19. Collins TJ, Berridge MJ, Lipp P, Bootman MD. Mitochondria are morphologically and functionally heterogeneous within cells. EMBO J. 2002 Apr 2; 21(7):1616–27. [PubMed: 11927546]

20. Riva A, Tandler B, Loffredo F, Vazquez E, Hoppel C. Structural differences in two biochemically defined populations of cardiac mitochondria. Am J Physiol Heart Circ Physiol. 2005 Aug; 289(2):H868–72. [PubMed: 15821034]

21. Duan JM, Karmazyn M. Acute effects of hypoxia and phosphate on two populations of heart mitochondria. Mol Cell Biochem. 1989 Oct 5; 90(1):47–56. [PubMed: 2608032]

22. Wollenbeerger A, Schulze W. Mitochondrial alterations in the myocardium of dogs with aortic stenosis. J Biophys Biochem Cytol. 1961 Jun 2; 10(3):285–8. [PubMed: 13786416]

23. Dabkowski ER, Baseler W, Williamson CL, Powell M, Razunguzwa TT, Frisbee JC, et al. Mitochondrial dysfunction in the type 2 diabetic heart is associated with alterations in spatially distinct mitochondrial proteomes. Am J Physiol Heart Circ Physiol. 2010 Aug; 299(2):H529–40. [PubMed: 20543078]

24. Ahmad T, Aggarwal K, Pattnaik B, Mukherjee S, Sethi T, Tiwari BK, et al. Computational classification of mitochondrial shapes reflects stress and redox state. Cell Death Dis Nature Publishing Group. 2013; 4(1):e461.

25. Reis Y, Bernardo-Faura M, Richter D, Wolf T, Brors B, Hamacher-Brady A, et al. Multi-parametric analysis and modeling of relationships between mitochondrial morphology and apoptosis. PLoS One. 2012; 7(1)

26. Akao M, O'Rourke B, Teshima Y, Seharaseyon J, Marbán E. Mechanistically distinct steps in the mitochondrial death pathway triggered by oxidative stress in cardiac myocytes. Circ Res. 2003; 92(2):186–94. [PubMed: 12574146]

27. Liu X, Hajnóczky G. Altered fusion dynamics underlie unique morphological changes in mitochondria during hypoxia-reoxygenation stress. Cell Death Differ. 2011; 18(10):1561–72. [PubMed: 21372848]

28. Lesnefsky EJ, Slabe TJ, Stoll MS, Minkler PE, Hoppel CL. Myocardial ischemia selectively depletes cardiolipin in rabbit heart subsarcolemmal mitochondria. Am J Physiol Heart Circ Physiol. 2001; 280(6):H2770–8. [PubMed: 11356635]

29. Dague, E., Genet, G., Lachaize, V., Guilbeau-Frugier, C., Fauconnier, J., Mias, C., et al. J Mol Cell Cardiol. Vol. 74. Elsevier Ltd; 2014 Sep. Atomic force and electron microscopic-based study of sarcolemmal surface of living cardiomyocytes unveils unexpected mitochondrial shift in heart failure; p. 162-72.

30. Sun J, Nguyen T, Aponte AM, Menazza S, Kohr MJ, Roth DM, et al. Ischaemic preconditioning preferentially increases protein S-nitrosylation in subsarcolemmal mitochondria. Cardiovasc Res. 2015 May; 106(2):227–36. [PubMed: 25694588]

31. Kurian GA, Berenshtein E, Saada A, Chevion M. Rat cardiac mitochondrial sub-populations show distinct features of oxidative phosphorylation during ischemia, reperfusion and ischemic preconditioning. Cell Physiol Biochem. 2012; 30(1):83–94. [PubMed: 22759958]

32. Hoppel CL, Tandler B, Fujioka H, Riva A. Dynamic organization of mitochondria in human heart and in myocardial disease. Int J Biochem Cell Biol. 2009 Oct; 41(10):1949–56. [PubMed: 19446651]

33. Sharp WW, Fang YH, Han M, Zhang HJ, Hong Z, Banathy A, et al. Dynamin-related protein 1 (Drp1)-mediated diastolic dysfunction in myocardial ischemia-reperfusion injury: therapeutic benefits of Drp1 inhibition to reduce mitochondrial fission. FASEB J. 2014 Jan; 28(1):316–26. [PubMed: 24076965]

34. Ong S-B, Subrayan S, Lim SY, Yellon DM, Davidson SM, Hausenloy DJ. Inhibiting mitochondrial fission protects the heart against ischemia/reperfusion injury. Circulation. 2010 May; 121(18):2012–22. [PubMed: 20421521]

35. Disatnik M-H, Ferreira JCB, Campos JC, Gomes KS, Dourado PMM, Qi X, et al. Acute inhibition of excessive mitochondrial fission after myocardial infarction prevents long-term cardiac dysfunction. J Am Heart Assoc. 2013 Oct.2(5):e000461. [PubMed: 24103571]

36. Shen AC, Jennings RB. Myocardial calcium and magnesium in acute ischemic injury. Am J Pathol. 1972 Jun; 67(3):417–40. [PubMed: 5033257]

37. Kloner RA, Fishbein MC, Braunwald E, Maroko PR. Effect of propranolol on mitochondrial morphology during acute myocardial ischemia. Am J Cardiol. 1978 May 1; 41(5):880–6. [PubMed: 645596]

38. Cellier L, Tamareille S, Kalakech H, Guillou S, Lenaers G, Prunier F, et al. Remote Ischemic Conditioning Influences Mitochondrial Dynamics. Shock. 2015; 45(2):1.

39. Vélez DE, Hermann R, Barreda Frank M, Mestre Cordero VE, Savino EA, Varela A, et al. Effects of wortmannin on cardioprotection exerted by ischemic preconditioning in rat hearts subjected to ischemia-reperfusion. J Physiol Biochem. 2016; 72(1):83–91. [PubMed: 26746207]

40. Zhao Z, Cui W, Zhang H, Gao H, Li X, Wang Y, et al. Pre-treatment of a single high-dose of atorvastatin provided cardioprotection in different ischaemia/reperfusion models via activating mitochondrial KATP channel. Eur J Pharmacol. 2015 Mar 15.751:89–98. [PubMed: 25641746]

- There are three subsets of cardiac mitochondria with unique shape parameters

- Ischemia induced morphological alterations in all three subsets of cardiac mitochondria

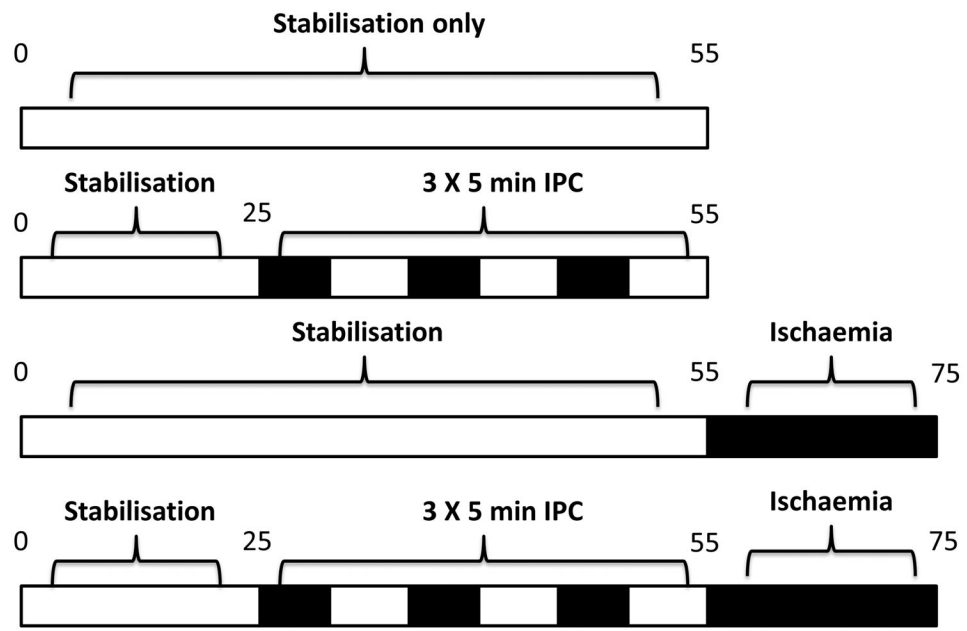- Ischemic preconditioning does not rescue their phenotype after ischemia

Figure 1. Experimental protocol
for exploring the effect of ST, ST+IPC, ST+IS and ST+IPC+IS on mitochondrial morphology. Times elapsed in minutes are shown above the bars.
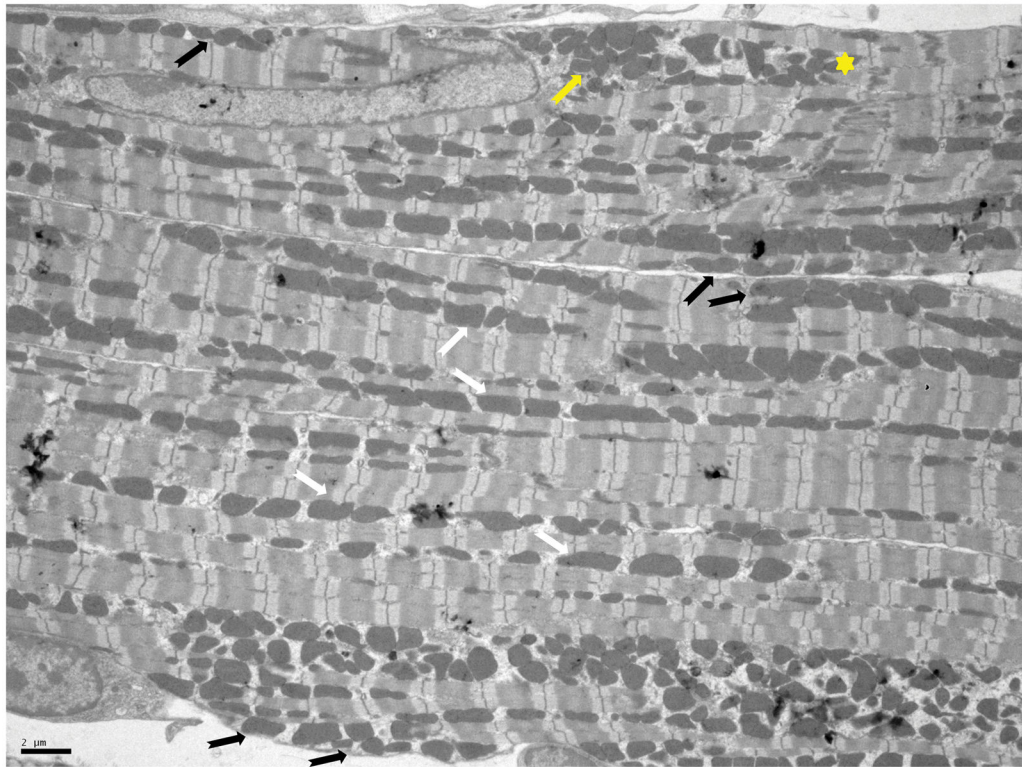
Figure 2. Three different subtypes of cardiac mitochondria
White arrows indicate the IMF mitochondria whereas the yellow and black arrows show the
PN and SSM mitochondria, respectively. The yellow star indicates the extent of spread of
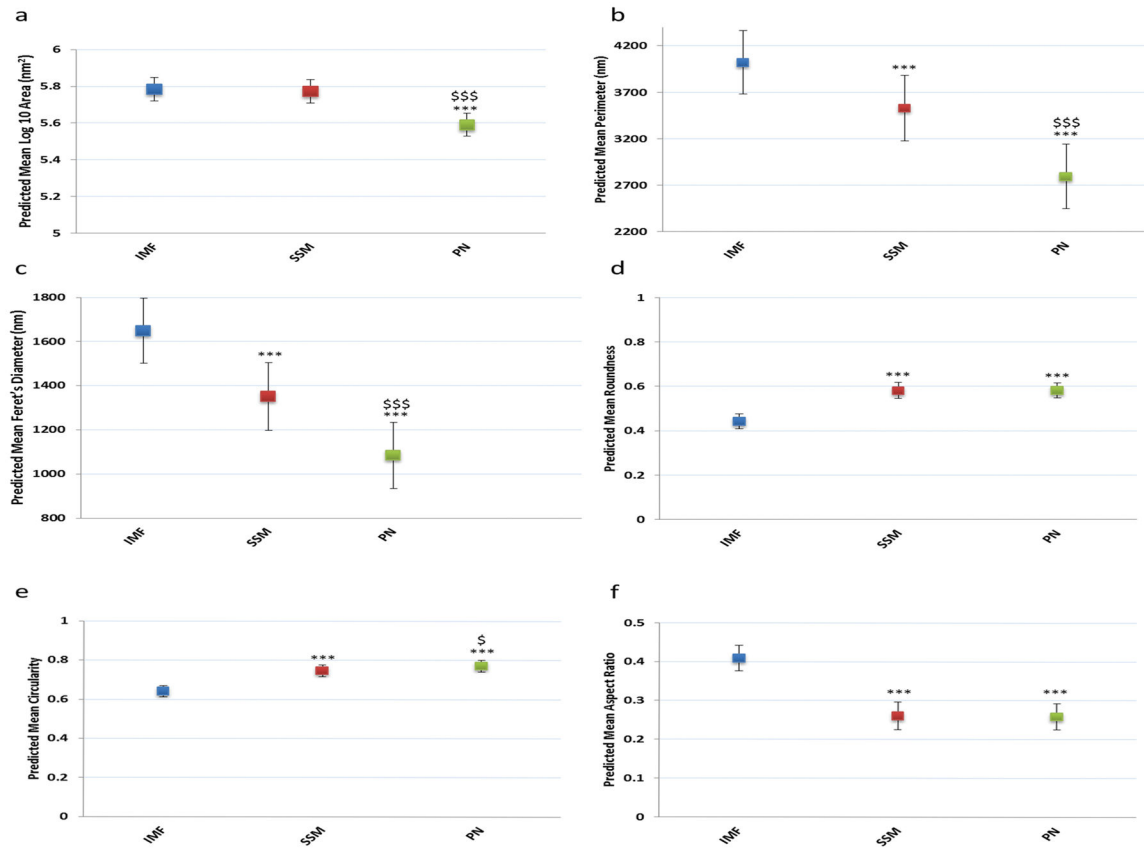PN mitochondria along the myofibers.

Figure 3. Morphological differences between subtypes of cardiac mitochondria
(a), (b) and (c) represent area, perimeter and Feret's diameter of different subtypes of
mitochondria whereas (d), (e) and (f) show roundness, circularity and AR of individual
mitochondria subtypes, respectively. *** denotes p<0.0001 for subsets compared to IMF
mitochondria and $$$ denotes p<0.0001 for the comparison of PN vs. SSM mitochondria
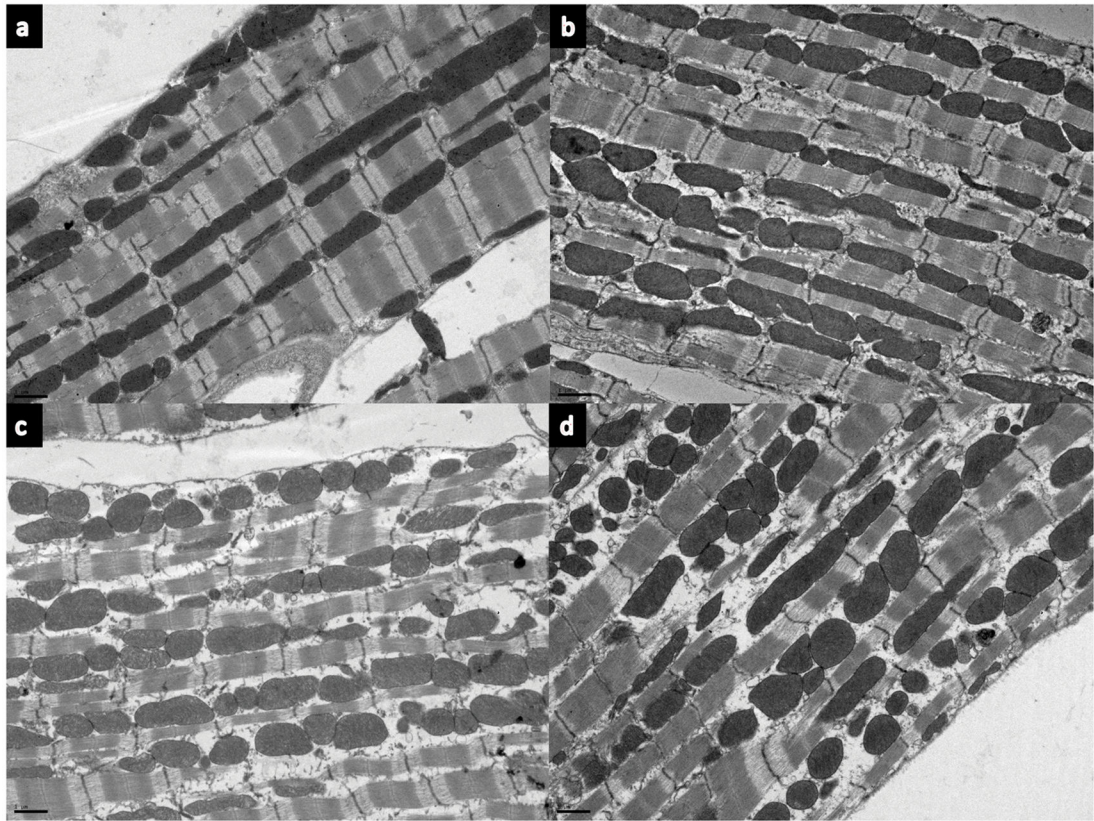(n=6 for each group).

Figure 4. Changes of IMF mitochondria after different treatments
(a) and (b) show the ST only or ST with IPC whereas (c) and (d) show the hearts treated with ischemia in the absence or presence of IPC, respectively.
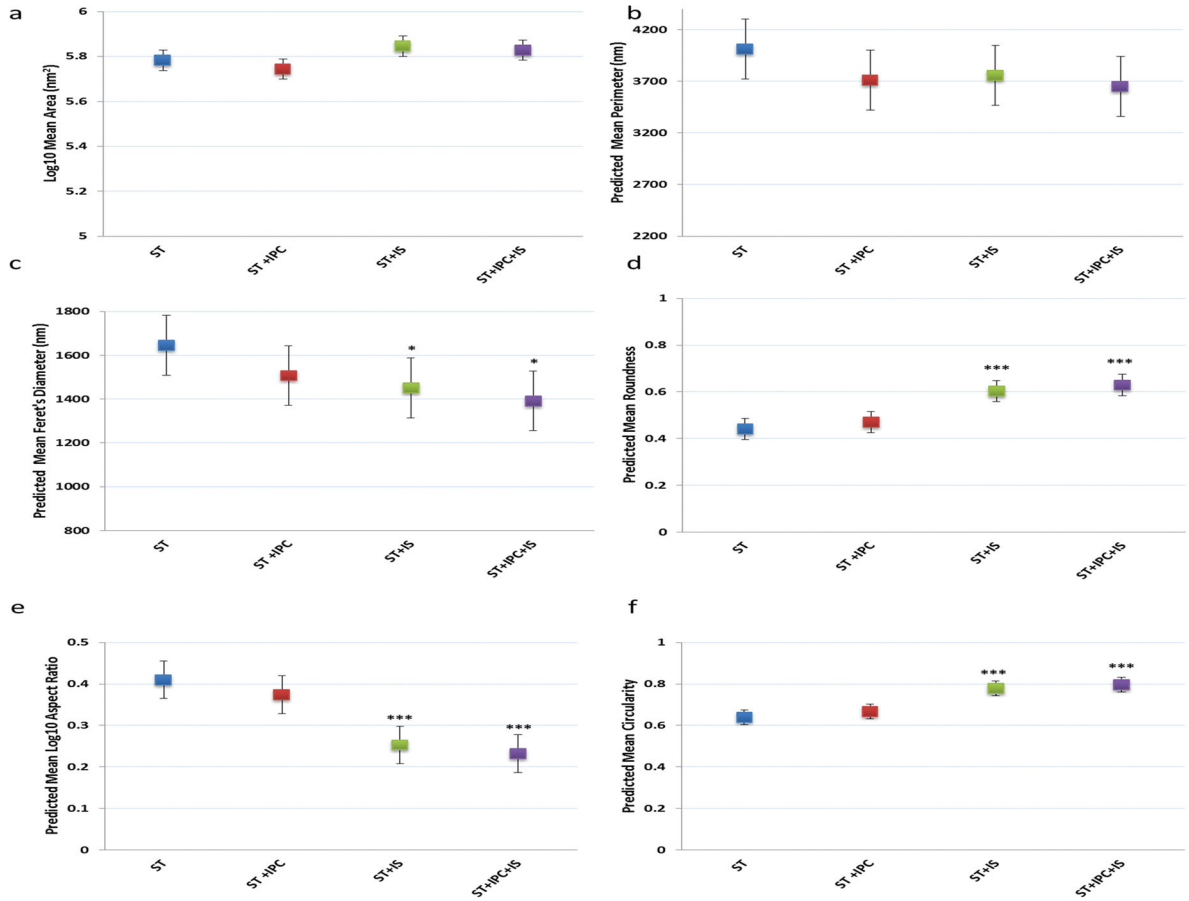
Figure 5. Morphological shape descriptors of IMF mitochondria after different treatments
(a), (b) and (c) represent area, perimeter and Feret's diameter of different subtypes of mitochondria whereas (d), (e) and (f) show roundness, circularity and AR of IMF subtype, respectively. * & *** denote $p<0.05$ and $p<0.0001$ for treatment compared to ST, respectively (ST = stabilization; IPC = ischemic preconditioning; IS = ischemia/n=6 for each group).
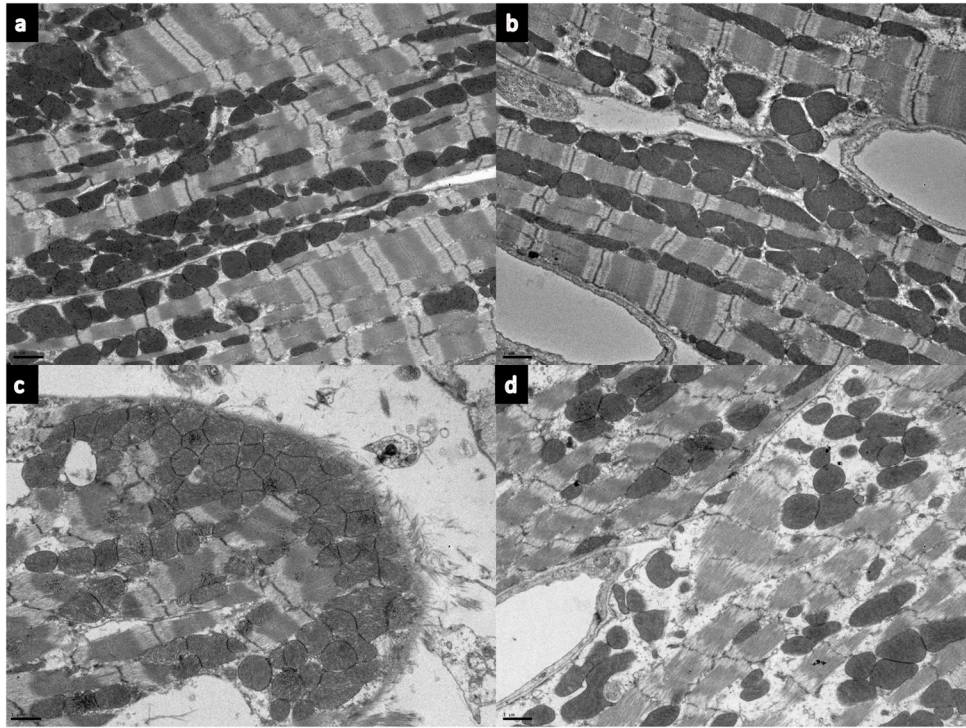
Figure 6. Morphological response of SSM mitochondria to different treatments
(a) and (b) images show the ST in the absence or presence of IPC whereas (c) and (d) show
the hearts treated with ischemia or with IPC prior to ischemia, respectively.
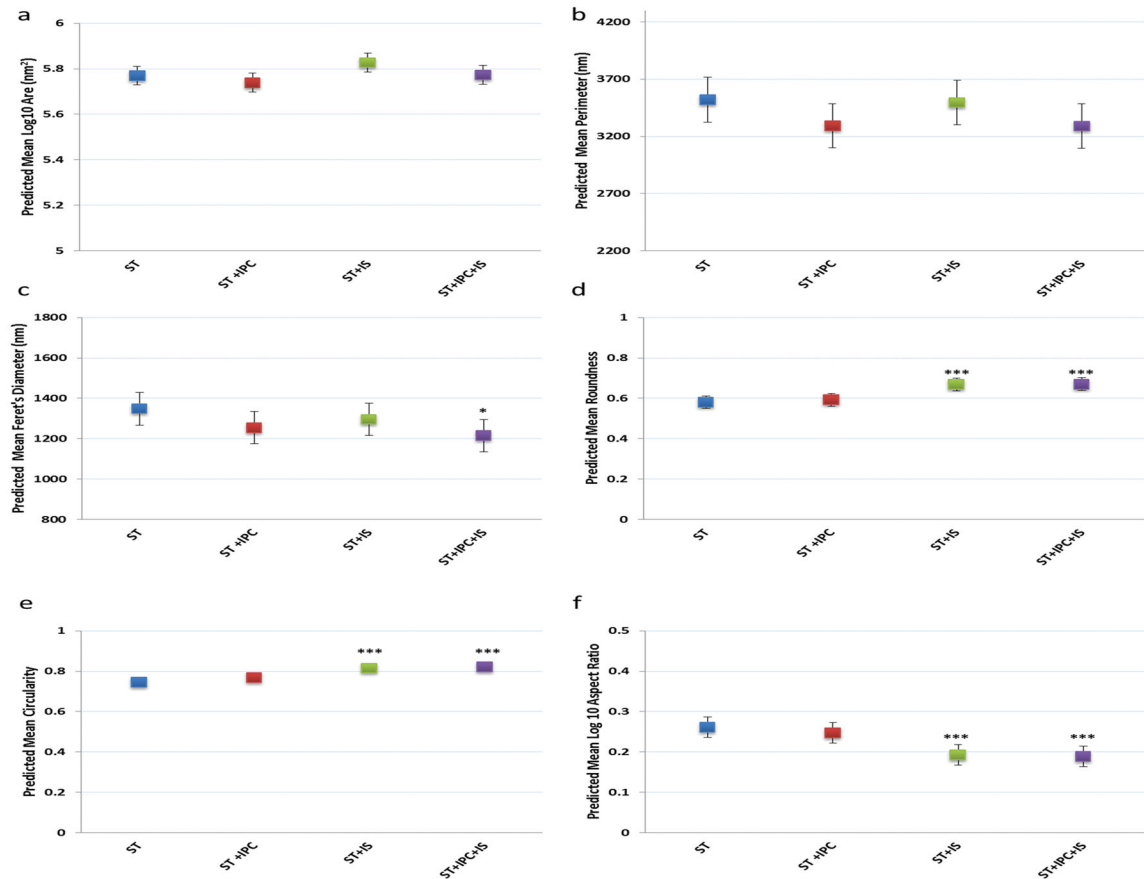
Figure 7. Alteration of SSM shape parameters after different treatments

(a), (b) and (c) graphs represent area, perimeter and Feret's diameter of SSM mitochondria whereas (d), (e) and (f) show roundness, circularity and AR of SSM mitochondria, respectively. * & *** denote p<0.05 and p<0.0001 for treatment compared to ST, respectively (ST = stabilization; IPC = ischemic preconditioning; IS = ischemia/n=6 for each group).
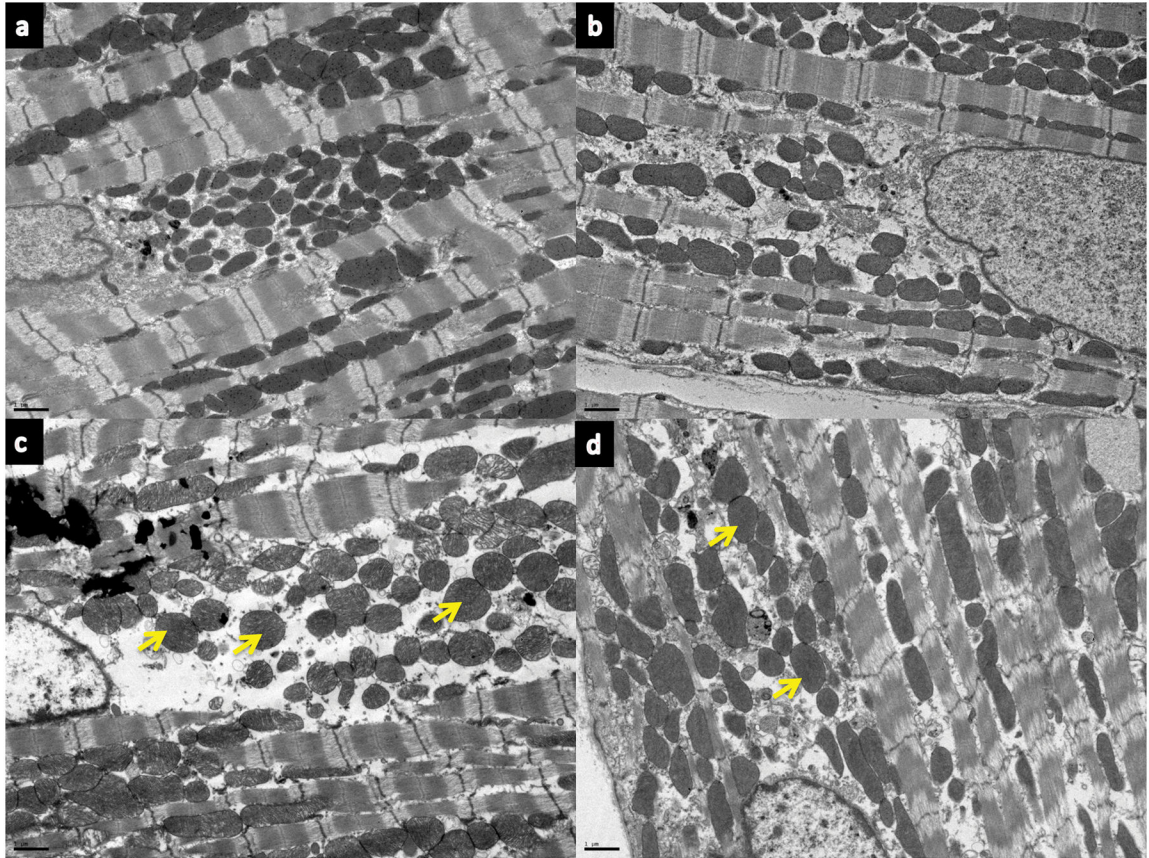
Figure 8. Alteration of PN mitochondria according to treatments
Panel (a) depicts ST and panel (b) depicts ST+ IPC. Panels (c) and (d) depict images from ischemia only or IPC + ischemia treatments, respectively. Yellow arrows indicate large globular PN mitochondria.
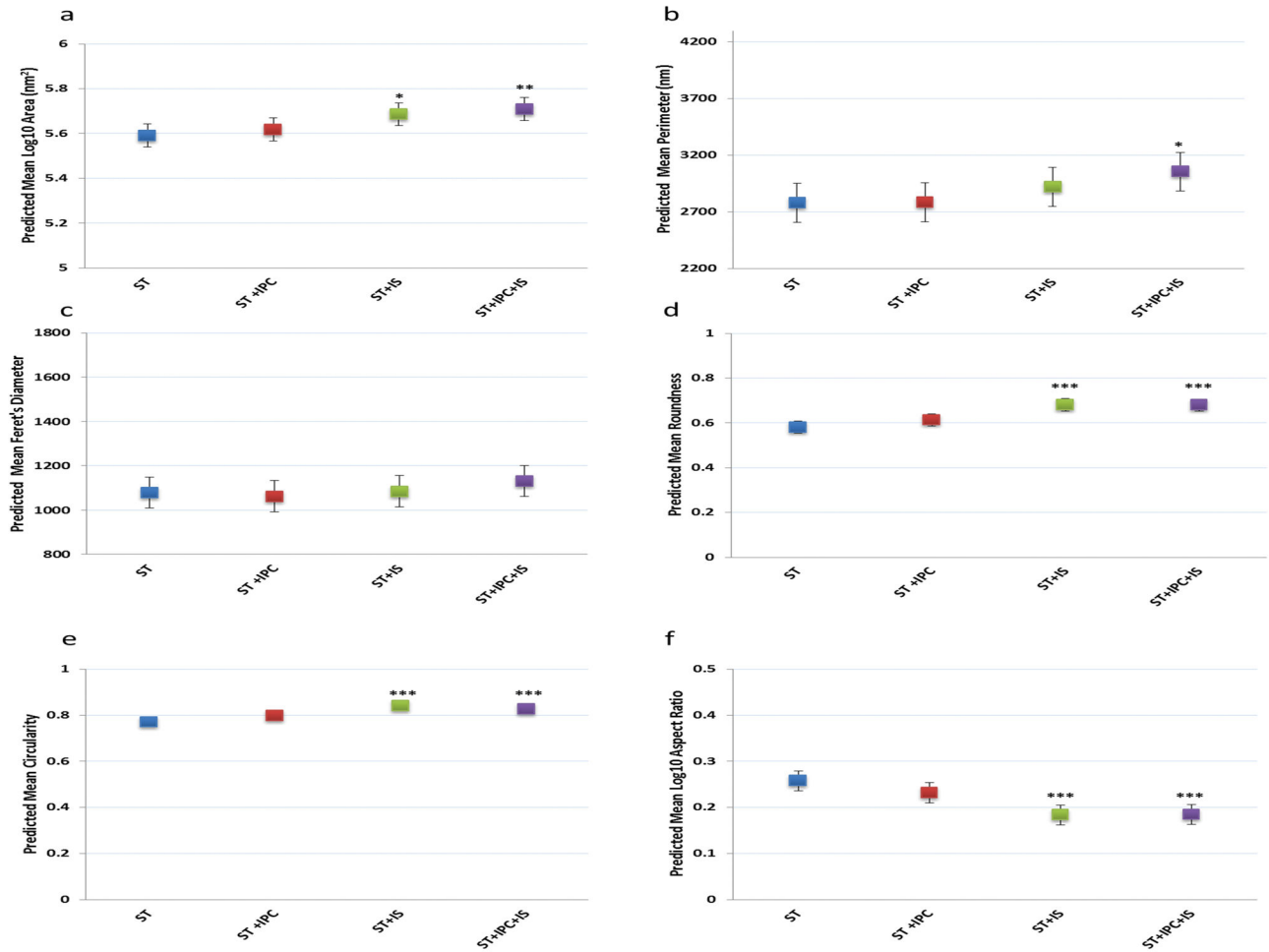
Figure 9. Shape parameter differences of PN mitochondria according to treatment groups
(a), (b) and (c) graphs represent area, perimeter and Feret's diameter of SSM mitochondria whereas (d), (e) and (f) show roundness, circularity and AR of PN mitochondria after different treatments, respectively. *, ** & *** denote $p < 0.05$, $p < 0.001$ and $p < 0.0001$ for treatment compared to ST, respectively (ST = stabilization; IPC = ischemic preconditioning; IS = ischemia/n=6 for each group).

Table 1

Comparison of predicted mean values ± S.E of different shape descriptors of Intermyofibrillar (IMF), Subsarcolemmal (SSM) and Perinuclear (PN) mitochondria at baseline (* and *** denote p 0.05 and p<0.0001, respectively).

Mitochondria Subtype	Log. Area	Perimeter	Feret's Diameter	Log. AR	Circularity	Roundness
IMF	5.78±0.32	4020.41±174.37	1648.70±75.25	0.41±0.02	0.64±0.02	0.44±0.02
vs.	vs.	vs.	vs.	vs.	vs.	vs.
SSM	5.77±0.33	3528.59±180.59***	1350.67±77.91***	0.26±0.02***	0.75±0.02***	0.58±0.02***
IMF	5.78±0.32	4020.41±174.37	1648.70±75.25	0.41±0.02	0.64±0.02	0.44±0.02
vs.	vs.	vs.	vs.	vs.	vs.	vs.
PN	5.59±0.32***	2793.21±177.22***	1084.10±76.47***	0.26±0.02***	0.77±0.02 ***	0.58±0.02 ***
SSM	5.77±0.33	3528.59±180.59	1350.67±77.91	0.26±0.02	0.75±0.02	0.58±0.02
vs.	vs.	vs.	vs.	vs.	vs.	vs.
PN	5.59±0.32***	2793.22±177.22***	1084.10±76.47***	0.26±0.02	0.77±0.02*	0.58±0.02

Table 2

Pairwise comparison of predicted mean values ± S.E of different shape descriptors of IMF mitochondria after individual treatments (* and *** denote p 0.05 and p<0.0001, respectively).

Specific Pairwise Analysis	Predicted Mean ± S.E for Different Shape Descriptors of IMF Mitochondria after Different Treatments					
	Log. Area	Perimeter	Feret's Diameter	Log.AR	Circularity	Roundness
(ST) vs. **(ST + IPC)**	5.78±0.02 vs. 5.74±0.02	4010.24±148.94 vs. 3710.97±147.96	1645.08±69.80 vs. 1507.18±69.4	0.41±0.02 vs. 0.37±0.02	0.64±0.02 vs. 0.67±0.02	0.44±0.02 vs. 0.47±0.02
(ST) vs. **(ST + IS)**	5.78±0.02 vs. 5.85±0.02	4010.24±148.94 vs. 3757.40±148.6	1645.08±69.80 vs. 1451.33±69.66*	0.41±0.02 vs. 0.25±0.02***	0.64±0.02 vs. 0.78±0.02***	0.44±0.02 vs. 0.60±0.02*
(ST) vs. **(ST + IPC+IS)**	5.78±0.02 vs. 5.83±0.02	4010.24±148.94 vs. 3647.89±148.41	1645.08±69.80 vs. 1391.62±69.58*	0.41±0.02 vs. 0.23±0.02***	0.64±0.02 vs. 0.80±0.02***	0.44±0.02 vs. 0.63±0.02*
(ST + IS) vs. **(ST+ IPC+ IS)**	5.85±0.02 vs. 5.83±0.02	3757.40±148.60 vs. 3647.89±148.41	1451.33±69.66 vs. 1391.62±69.58	0.25±0.02 vs. 0.23±0.02	0.80±0.02 vs. 0.80±0.02	0.60±0.02 vs. 0.63±0.02

Table 3

Pairwise comparison of predicted mean values ± S.E of different shape descriptors of SSM mitochondria after individual treatments (* and *** denote p 0.05 and p<0.0001, respectively).

Specific Pairwise Analysis	Predicted Mean ± S.E for Different Shape Descriptors of SSM Mitochondria after Different Treatments					
	Log. Area	Perimeter	Feret's Diameter	Log.AR	Circularity	Roundness
(ST) **Vs.** **(ST + IPC)**	5.77±0.02 vs. 5.74±0.02	3520.92±100.08 vs. 3292.36±98.82	1348.94±41.37 vs. 1254.75±40.91	0.26±0.01 vs. 0.25±0.01	0.75±0.01 vs. 0.77±0.01	0.58±0.02 vs. 0.59±0.02
(ST) **Vs.** **(ST + IS)**	5.77±0.02 vs. 5.83±0.02	3520.92±100.08 vs. 3495.68±99.48	1348.94±41.37 vs. 1295.90±41.16	0.26±0.01 vs. 0.20±0.01 ***	0.75±0.01 vs. 0.82±0.01 ***	0.58±0.02 vs. 0.67±0.02***
(ST) **Vs.** **(ST + IPC+IS)**	5.77±0.02 vs. 5.77±0.02	3520.92±100.08 vs. 3289.50±98.50	1348.94 ± 41.37 vs. 1215.07± 40.80*	0.26±0.01 vs. 0.19±0.01 ***	0.75±0.01 vs. 0.82±0.01 ***	0.58±0.02 vs. 0.67±0.02***
(ST + IS) **Vs.** **(ST+ IPC+ IS)**	5.83±0.02 vs. 5.77±0.02	3495.68±99.48 vs. 3289.50±98.50	1295.90±41.16 vs. 1215.07± 40.80	0.19±0.01 vs. 0.19±0.01	0.82±0.01 vs. 0.82±0.01	0.67±0.02 vs. 0.67±0.02

Table 4

Pairwise comparison of predicted mean values ± S.E of different shape descriptors of PN mitochondria after individual treatments (*, ** and*** denote p 0.05, p<0.001 and p<0.0001, respectively).

Specific Pairwise Analysis	Predicted Mean ± S.E for Different Shape Descriptors of PN Mitochondria after Different Treatments						
	Log. Area	Perimeter	Feret's Diameter	Log.AR	Circularity	Roundness
(ST) **Vs.** **(ST + IPC)**	5.59±0.03 vs. 5.62±0.03	2780.02±87.76 vs. 2783.01±87.27	1078.86±35.89 vs. 1062.37±35.70	0.26±0.01 vs. 0.23±0.01	0.77±0.01 vs. 0.80±0.01	0.58±0.01 Vs. 0.61±0.01
(ST) **Vs.** **(ST + IS)**	5.59±0.03 vs. 5.69±0.03 *	2780.02±87.75 vs. 2920.72±88.47	1078.86±35.90 vs. 1084.41±36.16	0.26±0.01 vs. 0.18±0.01 ***	0.77±0.01 vs. 0.84±0.01***	0.58±0.01 Vs. 0.68±0.01***
(ST) **Vs.** **(ST + IPC+IS)**	5.59±0.03 vs. 5.71±0.03 **	2780.02±87.75 vs. 3055.42±86.95 *	1078.86±35.90 vs. 1131.47± 35.58 *	0.26±0.01 vs. 0.19±0.01 ***	0.77±0.01 vs. 0.83±0.01***	0.58±0.01 vs. 0.68±0.01***
(ST + IS) **Vs.** **(ST+ IPC+ IS)**	5.69±0.03 vs. 5.71±0.03	2920.72±88.47 vs. 3055.42±86.95	1084.41±36.16 vs. 1131.47 ± 35.58	0.18±0.01 vs. 0.19±0.01	0.84±0.01 vs. 0.83±0.01	0.68±0.01 Vs. 0.68±0.01